Optical Materials 34 (2012) 959–964

Contents lists available at ScienceDirect

Optical Materials

journal homepage: www.elsevier.com/locate/optmat

Investigation of continuous-wave and Q-switched microchip laser characteristics of Yb:YAG ceramics and crystals

Jun Dong [a,b,*], Guozhang Xu [a], Jian Ma [a], Mengjun Cao [a], Ying Cheng [a], Ken-ichi Ueda [b], Hideki Yagi [c], Alexander A. Kaminskii [d]

[a] Department of Electronics Engineering, Xiamen University, Xiamen 361005, China
[b] Institute for Laser Science, University of Electro-Communications, 1-5-1 Chofugaoka, Chofu, Tokyo 182-8585, Japan
[c] Konoshima Chemical Co., Ltd., 80 Kouda, Takuma, Mitoyo-gun, Kagawa 769-1103, Japan
[d] Institute of Crystallography, Russian Academy of Sciences, Moscow 119333, Russia

ARTICLE INFO

Article history:
Received 30 January 2011
Received in revised form 27 April 2011
Accepted 4 May 2011
Available online 28 May 2011

Keywords:
Yb:YAG
Ceramics
Single-crystal
Passively Q-switched
Polarization states

ABSTRACT

Continuous-wave and passively Q-switched microchip laser performance of Yb:YAG ceramics and single-crystals was investigated. Highly efficient continuous-wave Yb:YAG laser performance was observed at 1030 nm and 1049 nm for both Yb:YAG ceramics and crystals with different transmissions of output couplers. The laser performance of Yb:YAG ceramic is comparable to that of Yb:YAG single crystal. Meanwhile, the laser performance of laser-diode pumped Yb:YAG/Cr^{4+}:YAG all-ceramics- and all-crystals-combination passively Q-switched microchip lasers were investigated. Sub-nanosecond laser pulses with peak power over 150 kW were obtained with different Yb:YAG/Cr^{4+}:YAG combinations. Linearly polarized laser was observed in Yb:YAG/Cr^{4+}:YAG all-crystals combination and circular polarized laser was obtained in Yb:YAG/Cr^{4+}:YAG all-ceramics combination. The best laser performance was obtained with Yb:YAG/Cr^{4+}:YAG all-crystals combination.

1. Introduction

Ytterbium doped laser materials have been intensely investigated for developing high power laser-diode pumped solid-state lasers around 1 μm [1]. Yb:YAG as crystals and polycrystalline ceramics are one of the dominant laser gain media used for solid-state lasers [2–6] owing to the excellent optical, thermal, chemical and mechanical properties [2]. Owing to the small radius difference between yttrium ions and ytterbium ions [3], Yb:YAG single-crystal doped with different Yb concentrations can be grown by different crystal growth methods and efficient laser performance has been achieved [4–6]. By introducing Cr ions into Yb:YAG crystal, Cr, Yb:YAG self-Q-switched laser crystal was grown successfully and efficient laser operation was achieved in Cr, Yb:YAG self-Q-switched laser crystal pumped by laser-diode [4]. Transparent laser ceramics [5–9] fabricated by the vacuum sintering technique and nanocrystalline technology [10] have been proven to be potential replacements for their counterpart single crystals because they have several remarkable advantages such as high concentration and easy fabrication of large-size ceramics, fabrication of multilayer and multifunctional ceramics laser materials [11,12]. Efficient and high power laser operation in Nd^{3+}- and Yb^{3+}-ions doped YAG ceramics has been demonstrated [7,8]. Passively Q-switched Yb:YAG/Cr^{4+}:YAG all-ceramics microchip lasers with high peak power and sub-nanosecond pulse width have been reported [13–15]. Yb:YAG laser materials have become promising candidates for high-power laser-diode pumped solid-state lasers with rod [16], slab [17], and thin disk [18,19] configurations. The quasi-three-level laser system of Yb:YAG requires high pumping intensity to overcome transparency threshold and to achieve efficient laser operation at room temperature [20]. The thin disk laser has been demonstrated to be a good way to generate high power with good beam quality owing to the efficiently cooling of gain medium and good overlap of the pump beam and laser beam [18]. However, in the thin disk case, the pump beam must be folded many times into thin laser gain medium with mirrors in order to absorb sufficient pump power, which makes the laser system extremely complicated. Some applications require that the lasers should be compact and economic; the cooling system should be eliminated in compact and easily maintainable laser system. Therefore, laser-diode end-pumped microchip lasers are a better choice to achieve highly efficient laser operation under high pump power intensity. The thinner the gain medium, the better the cooling effect, therefore, heavy doped Yb:YAG gain media are the better choice for such lasers. The development of Yb:YAG ceramics doped with 1 at.% Yb^{3+} ions has been reported [9], but the efficiency of such Yb:YAG ceramic laser is low owing to the deficient activator concentration. In principle, there is no concentration quenching

* Corresponding author at: Department of Electronics Engineering, Xiamen University, Xiamen 361005, China. Tel.: +86 592 2580196; fax: +86 592 2580040.
E-mail address: jdong@xmu.edu.cn (J. Dong).

0925-3467/$ - see front matter © 2011 Elsevier B.V. All rights reserved.
doi:10.1016/j.optmat.2011.05.005

effect in Yb:YAG, however, the unwanted impurities (such as Er^{3+}, Tm^{3+}, Ho^{3+}, and so on) from raw materials will be deleterious to the laser performance owing to the high activator doping. Concentration dependent optical properties and laser performance of Yb:YAG crystals have been reported [21–24]. The concentration quenching of Yb:YAG crystals has been investigated and it was found that fluorescence lifetime decreases when the Yb concentration is higher than 15 at.% and lifetime decreases up to 15% when the Yb concentration reaches to 25 at.% [22,25]. Optical spectra of Yb:YAG ceramics doped with different Yb^{3+}-lasant concentration (C_{Yb} = 9.8, 12, and 20 at.%) and efficient 9.8 at.% Yb:YAG ceramic microchip lasers [8] have been reported recently. The comparison of laser performance of Yb:YAG ceramic and single-crystals doped with 20 at.% Yb has been reported [26]. And systematic comparison studies of miniature laser performance of Yb:YAG ceramics and single-crystals doped with different Yb concentrations were reported recently [27].

In this paper, we present our recent investigations of continuous-wave (cw) and passively Q-switched microchip laser performance of Yb:YAG crystals and ceramics doped with 10 at.% Yb. The comparison of the continuous-wave laser performance of microchip Yb:YAG ceramic and crystal lasers at 1030 nm and 1049 nm was conducted with different output couplings. Efficient laser at 1030 nm and 1049 nm with different output couplings was achieved with Yb:YAG crystals and ceramics. Multi-longitudinal-mode oscillations were observed in these Yb:YAG microchip lasers. Yb:YAG ceramics show comparable laser performance to their crystal counterparts. Efficient, sub-nanosecond pulse width and high peak power passively Q-switched laser pulses were generated in Yb:YAG/Cr^{4+}:YAG all-crystals and all-ceramics combinations. Linearly polarized laser output was observed in Yb:YAG/Cr^{4+}:YAG all-crystals combination, while circularly polarized laser output was achieved in Yb:YAG/Cr^{4+}:YAG all-ceramics combination.

2. Experimental

Yb:YAG and Cr^{4+}:YAG ceramics used in experiments were fabricated by the vacuum sintering technique and nanocrystalline technology, and Yb concentration is 9.8 at.%. Counterpart Yb:YAG and Cr^{4+}:YAG crystals used in experiments were grown by Czochralski (CZ) method along the [1 1 1] direction, and Yb ions doping concentration is 10 at.%. The thickness of Yb:YAG and Cr^{4+}:YAG samples was set to be 1 mm for comparing the laser performance. Initial transmission of Cr^{4+}:YAG samples was measured to be 80% for comparing the performance of passively Q-switched Yb:YAG/Cr^{4+}:YAG microchip lasers.

To compare the continuous-wave and Q-switched laser performance of Yb:YAG ceramics and single-crystals, microchip lasers were used in the experiments. Fig. 1 shows a schematic diagram of the experimental setup for laser-diode pumped Yb:YAG microchip laser and passively Q-switched Yb:YAG/Cr^{4+}:YAG microchip laser. One surface of the Yb:YAG samples was coated for antireflection at 940 nm and high reflection at 1.03 μm to act as the rear cavity mirror, the other surface was coated for antireflection at 1.03 μm to reduce the intracavity loss. Plane-parallel fused silica output couplers with transmission (T_{oc}) of 5%, 10%, 15%, and 20% were mechanically attached to the gain medium tightly. For comparison of the laser performance of passively Q-switched Yb:YAG/Cr^{4+}:YAG microchip laser, saturable absorber Cr^{4+}:YAG samples were sandwiched between Yb:YAG sample and output coupler acting as Q-switch. Plane-parallel fused silica output coupler with 50% transmission was used in the experiments. Total cavity length was 2 mm.

A high-power fiber-coupled 940 nm laser diode with a core diameter of 100 μm and numerical aperture of 0.22 was used as

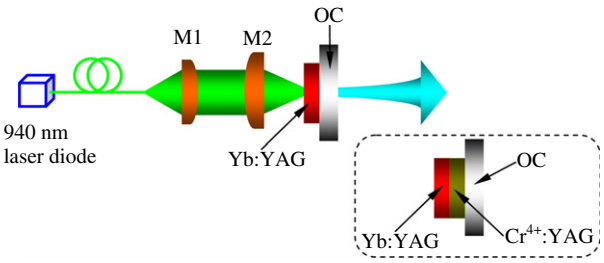

Fig. 1. Schematic diagram of laser-diode pumped Yb:YAG ceramics and crystals microchip lasers. OC, output coupler; M1, focus lens with focal length of 8 mm; M2, focus lenses with different focal lengths. Dotted frame shows the experimental setup for passively Q-switched Yb:YAG/Cr^{4+}:YAG microchip laser.

the pump source. One lens with 8 mm focal length was used to collimate pump laser, and other lens with different focal lengths (12 mm focal length for continuous-wave laser, and 8 mm focal length for Q-switched laser) were used to focus the pump beam on the Yb:YAG rear surface. After the coupling optics, there is about 95% pump power incident on the Yb:YAG samples and the pump light spot in Yb:YAG sample is about 120 μm in diameter for continuous-wave operation and 100 μm in diameter for Q-switched laser operation. The laser was operated at room temperature. The Q-switched pulse profiles were recorded by using a fiber-coupled InGaAs photodiode with a bandwidth of 16 GHz, and a 7 GHz Tektronix TDS7704B digital phosphor oscilloscope. The laser spectrum was analyzed by using an optical spectrum analyzer. The laser output beam profile was monitored using a CCD camera both in the near-field and the far-field of the output coupler. The polarization states of these microchip lasers were determined by using a Glan-Thomson prism and a power meter.

3. Results and discussion

Fig. 2 shows the cw output power of Yb:YAG ceramics and single-crystals microchip lasers as a function of the absorbed pump power for different T_{oc}. The absorbed pump power threshold for Yb:YAG ceramic increases from 200 mW to 350 mW with T_{oc}, which are higher than those for Yb:YAG crystal (0.14, 0.26, 0.3, and 0.32 W for T_{oc} = 5%, 10%, 15% and 20% respectively). The output power increases linearly with the absorbed pump power for Yb:YAG ceramic sample when the absorbed pump power is well above the pump power threshold, which is the nature of quasi-three-level system of Yb:YAG; the high efficiency can be achieved by using high pump power intensity at room temperature [28]. For T_{oc} = 5%, the laser operates at 1030 nm when the absorbed pump power is above the pump power threshold and is kept below 0.65 W for Yb:YAG ceramic; the laser operates at 1030 nm and 1049 nm simultaneously when the absorbed pump power is kept between 0.65 W and 0.9 W, as shown in Fig. 2a. The output power increases rapidly with absorbed pump power due to oscillation of 1049 nm during dual-wavelength operation as shown in the inset of Fig. 2a. The laser operates at 1049 nm when the absorbed pump power is higher than 0.9 W. The same situation was also observed in Yb:YAG single-crystal microchip laser with T_{oc} = 5%, the difference is that the threshold for 1030 nm oscillation is lower and dual-wavelength oscillation is in the absorbed pump power range of 0.55 and 0.75 W. The slope efficiency for 1049 nm is 64% for Yb:YAG ceramic and 81% for Yb:YAG crystal. Maximum output power at 1049 nm is 3.8 W for Yb:YAG ceramic and 4.3 W for Yb:YAG crystal at absorbed pump power of 6.5 W; the corresponding optical-to-optical efficiencies are 59% and 66% for Yb:YAG ceramic and crystal, respectively. There is a tendency of saturation for Yb:YAG crystal at high pump power level, and there

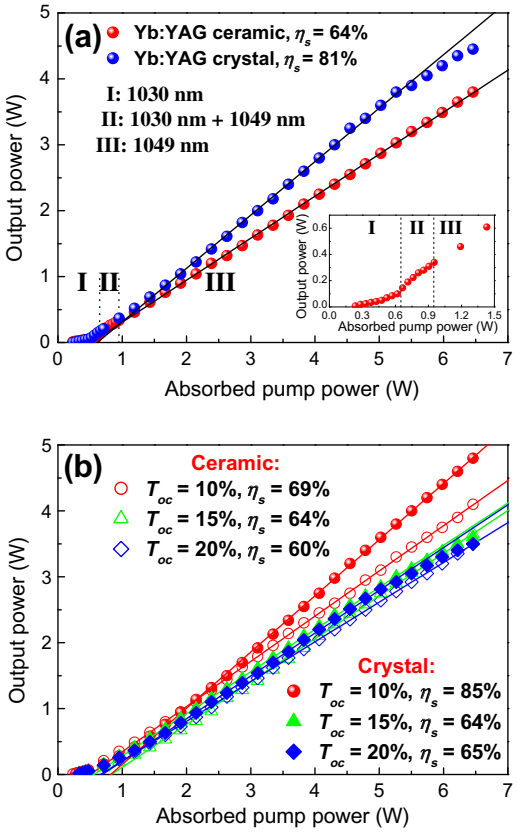

Fig. 2. Output power for (a) T_{oc} = 5%, and (b) T_{oc} = 10%, 15%, and 20% for Yb:YAG ceramic and crystal microchip lasers as a function of absorbed pump power. Insert in Fig. 2a shows the absorbed pump power range for different wavelength oscillations for Yb:YAG ceramics.

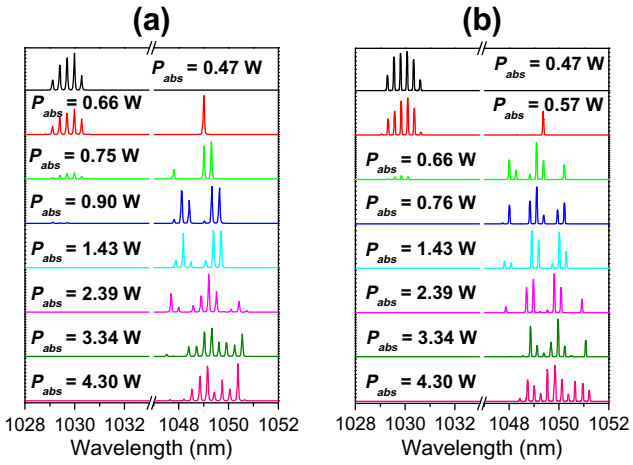

Fig. 3. Laser emitting spectra of Yb:YAG ceramic (a) and crystal (b) microchip lasers for T_{oc} = 5% under different pump power levels. The resolution of the optical spectral analyzer is 0.01 nm.

is no saturation effect for Yb:YAG ceramic and high power can be further scaled by increasing the pump power.

For T_{oc} is 10% or higher, the laser of Yb:YAG ceramic and crystal operates only around 1030 nm. The best laser performance was obtained with T_{oc} = 10% for both Yb:YAG ceramic and crystal. The slope efficiencies of Yb:YAG ceramic lasers are 69%, 64%, and 60% for T_{oc} = 10%, 15% and 20%, respectively. The slope efficiencies of Yb:YAG crystal lasers are 85%, 64%, and 65% for T_{oc} = 10%, 15% and 20%, respectively. Maximum output power of 4 W at 1030 nm for Yb:YAG ceramic is obtained with T_{oc} = 10% when the absorbed pump power is 6.5 W; the corresponding optical-to-optical efficiency is 62%. And maximum output power of 4.6 W at 1030 nm for Yb:YAG crystal is obtained with T_{oc} = 10% when the absorbed pump power is 6.5 W; the corresponding optical-to-optical efficiency is 74%. For Yb:YAG ceramic, although the laser performance is not good as that of Yb:YAG crystal for different transmissions of output coupler, the output power is not saturated for different transmissions of output coupler, which can be further scaled by increasing pump power. For Yb:YAG crystal, except for T_{oc} = 10%, there is a saturation effect with pump power at high pump power level. These prove that the thermal effect of Yb:YAG ceramic is better than that of Yb:YAG crystal. The inferior performance of Yb:YAG ceramic is maybe caused by the poor optical quality of Yb:YAG ceramic comparing to that of Yb:YAG crystal, the optical quality of Yb:YAG ceramics can be further improved by adjusting the ceramic sintering process.

The laser spectra of these lasers indicate several longitudinal modes oscillate simultaneously (around 1049 nm for T_{oc} = 5% when absorbed pump power is higher than 0.9 W for Yb:YAG ceramic and 0.75 W for Yb:YAG crystal; and around 1030 nm for both Yb:YAG crystal and ceramic for T_{oc} = 10%, 15% and 20%, respectively). Fig. 3 shows the laser emitting spectra of Yb:YAG ceramic and crystal microchip lasers under different absorbed pump power for T_{oc} = 5%. For T_{oc} = 5%, multi- longitudinal modes oscillate at 1030 nm when the pump power is just over threshold, while number of the longitudinal modes increases with further increase of the pump power when absorbed pump power is kept lower than 0.65 W for Yb:YAG ceramic (as shown in Fig. 3a) and 0.55 W for Yb:YAG crystal (as shown in Fig. 3b). Dual-wavelength oscillation was observed when the absorbed pump power was kept between 0.65 W and 0.9 W for Yb:YAG ceramic, and between 0.55 and 0.75 W for Yb:YAG crystal. The intensity and number of longitudinal modes around 1030 nm decrease and the intensity and number of longitudinal modes around 1049 nm increase with the absorbed pump power when the laser oscillates in the dual-wavelength region. The laser spectra show that Yb:YAG laser oscillates around 1049 nm when the absorbed pump power is above 0.9 W for Yb:YAG ceramic, and above 0.75 W for Yb:YAG crystal. The number of longitudinal modes around 1049 nm increases with absorbed pump power (as shown in Fig. 3). The separation of two close longitudinal modes is measured to be 0.3 nm, which is in good agreement with the free spectral range (0.292 nm) of 1 mm long cavity filled with gain medium predicted by [29] $\Delta\lambda_c = \lambda^2/2L_c$, where L_c is the optical length of the resonator and λ is the laser wavelength. And the center wavelength of the lasers shifts to longer wavelength with the pump power which is caused by the temperature dependent emission spectra of Yb:YAG crystal [30]. The cause of switching of laser wavelength and dual-wavelength operation for Yb:YAG ceramic and crystal laser with T_{oc} = 5% is attributed to the quasi-three level nature of Yb:YAG material and the local temperature rise due to the heat generated at high pump power. The local temperature rise inside Yb:YAG gain medium has a great effect on the thermal population distribution of terminated laser level for 1030 nm, the reabsorption around the strong emission peak of 1030 nm increases, the threshold for 1030 nm oscillation increases. However, the local temperature rise has little effect on the reabsorption loss around the weak emission peak of 1049 nm for Yb:YAG gain medium, there is a tradeoff between 1030 nm and 1049 nm oscillations. With further increase of the local temperature, the reabsorption loss at 1030 nm increases, the laser prefers to oscillate at 1049 nm than at 1030 nm with T_{oc} = 5%.

For T_{oc} = 10%, 15%, and 20%, the lasers oscillate only around 1030 nm, and the number of oscillating longitudinal modes was found to increase from three, just above threshold, to eight at

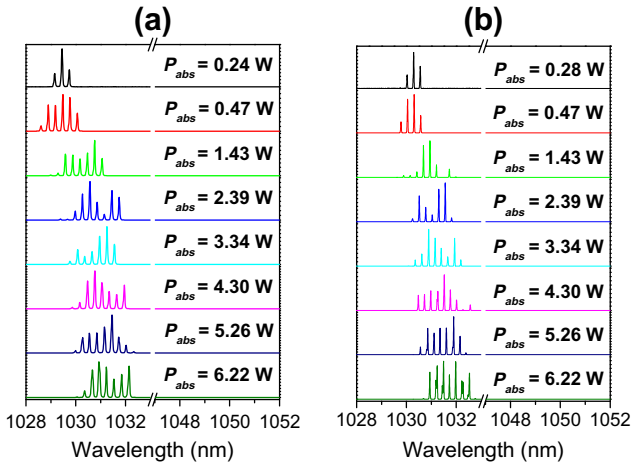

Fig. 4. Laser emitting spectra of Yb:YAG ceramic (a) and crystal (b) microchip lasers for T_{oc} = 10% under different pump power levels. The resolution of the optical spectral analyzer is 0.01 nm.

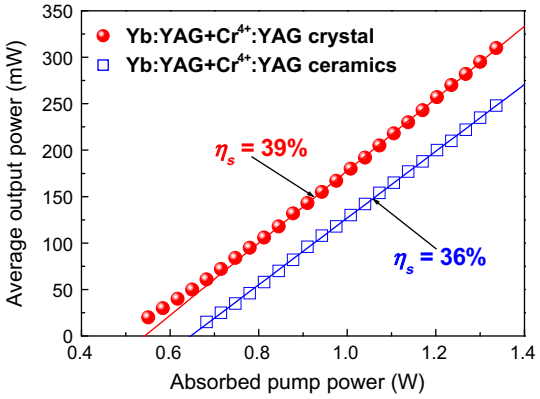

Fig. 5. Average output power of passively Q-switched Yb:YAG/Cr^{4+}:YAG microchip lasers as a function of the absorbed pump power. The solid lines show the linear fits of the experimental data.

higher pump power. Fig. 4 shows the laser emitting spectra of Yb:YAG ceramic and crystal microchip lasers for T_{oc} = 10% under different absorbed pump power. The separation of each longitudinal mode under different pump power was about 0.29 nm. The linewidth of each mode was measured to be less than 5.7 GHz, i.e. the resolution limit of the instrument.

The number of longitudinal modes increases with the absorbed pump power because the inversion population provided with pump power can overcome the threshold for low gain away from the highest emission peak of Yb:YAG gain medium. The longitudinal mode oscillation for these microchip Yb:YAG lasers was mainly caused by the etalon effect of plane-parallel Yb:YAG thin plate. For T_{oc} = 5%, both Yb:YAG ceramic and crystal lasers are oscillating at longer wavelength comparing to those for T_{oc} = 10%. The cause of the wavelength shift to longer wavelength for T_{oc} = 5% is related to the change of the intracavity laser intensity [31] because only the intracavity laser intensity is different for both cases. Intracavity laser intensity for T_{oc} = 5% is about two times higher than that for T_{oc} = 10%, therefore, more longitudinal modes will also be excited for T_{oc} = 5%. Because the better laser performance for Yb:YAG crystal lasers was obtained comparing with that of Yb:YAG ceramics lasers, the intracavity intensity is higher for crystal laser, therefore Yb:YAG crystal lasers oscillate at longer wavelength than those for Yb:YAG ceramics lasers, especially for T_{oc} = 5%. Strong mode competition and mode hopping in these Yb:YAG microchip lasers were also observed. When the laser oscillates, the excited Yb^{3+} ions jump back to the lower laser level, they always relax to other even-lower energy levels or ground level, this process is rapid compare to the lifetime of Yb^{3+} ion in YAG crystal or ceramics. The relaxation of Yb^{3+} ions to the lower energy or ground levels causes the lower-level population to increase with the lasing intensity, which increases the reabsorption. This enhanced reabsorption provides a negative feedback process for the lasing modes and effective gain profile of Yb:YAG medium. This negative feedback process accompanied with the effects of strong mode competition makes some stronger laser modes eventually faded or quenched. When the intracavity light intensity is high enough, the population distribution at lower energy levels is changed dramatically. At the same time, the effective gain curve of Yb:YAG under lasing condition was altered by the strong reabsorption and temperature rise induced by the absorbed pump power. Some initially suppressed modes at longer wavelength governed by the emission spectra can oscillate under changed gain curve, therefore the laser wavelength shifts to longer wavelength and mode hopping was observed.

Comparison of the laser performance of Yb:YAG/Cr^{4+}:YAG microchip lasers was done by inserting a 1 mm thick Cr^{4+}:YAG between Yb:YAG and output coupler. Average output power Yb:YAG/Cr^{4+}:YAG microchip lasers as a function of absorbed pump power was shown in Fig. 5. The absorbed pump power thresholds were about 0.53 and 0.66 W for Yb:YAG/Cr^{4+}:YAG all-crystals combination and all-ceramics combination, respectively. The higher pump power threshold of these passively Q-switched lasers was due to the low initial transmission of Cr^{4+}:YAG and high transmission of the output coupler used in the experiments. Average output power increases linearly with absorbed pump power for these microchip lasers, the slope efficiencies with respect to the absorbed pump power were estimated to be about 39%, 36%, for Yb:YAG/Cr^{4+}:YAG all-crystals combination and all-ceramics combination, respectively. The best laser performance (low threshold and high slope efficiency) of passively Q-switched Yb:YAG/Cr^{4+}:YAG microchip lasers was obtained with Yb:YAG/Cr^{4+}:YAG all-crystals combination because of the enhancement of linearly polarized laser operation due to the combination of nonlinear saturation absorption effects of Cr^{4+}:YAG crystal under high intracavity laser intensity [32] and the crystalline-orientation selected linearly polarized states of Yb:YAG crystal [33]. Maximum average output power of 310 mW and 248 mW was obtained with Yb:YAG/Cr^{4+}:YAG all-crystals and all-ceramics combinations respectively when the absorbed pump power was 1.34 W, corresponding to optical-to-optical efficiency of 23%, and 18.5%. There is no coating damage occurrence with further increase of the pump power owing to decrease of the intracavity energy fluence by using high transmission output coupler.

Fig. 6 shows the typical pulse profile of passively Q-switched Yb:YAG/Cr^{4+}:YAG microchip lasers with Yb:YAG/Cr^{4+}:YAG all-crystals and all-ceramics combinations when the absorbed pump power of 1.34 W was applied. The pulse profile of all-crystals combination is symmetry while the pulse profile of all-ceramics combination is not symmetry, the pulse rise time is shorter than pulse fall time. The shortest pulse width of 282 ps was achieved with Yb:YAG/Cr^{4+}:YAG all-crystals combination and 337 ps was achieved with Yb:YAG/Cr^{4+}:YAG all-ceramics combination when the absorbed pump power of 1.34 W was applied. The corresponding peak power of 215 kW and 150 kW was obtained for Yb:YAG/Cr^{4+}:YAG all-crystals and all-ceramics combinations, respectively. Fig. 7 shows the pulse characteristics (pulse repetition rate, pulse width, pulse energy and pulse peak power) of passively Q-switched Yb:YAG/Cr^{4+}:YAG microchip lasers as a function of absorbed pump power. For both Yb:YAG/Cr^{4+}:YAG all-ceramics and all-crystals combinations, the repetition rate of passively Q-switched lasers increases linearly with the absorbed pump power. Pulse width (FWHM) of passively Q-switched Yb:YAG/Cr^{4+}:YAG microchip

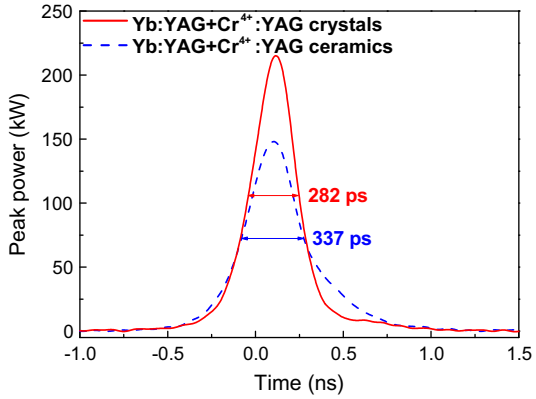

Fig. 6. Pulse profiles of passively Q-switched Yb:YAG/Cr^{4+}:YAG microchip lasers.

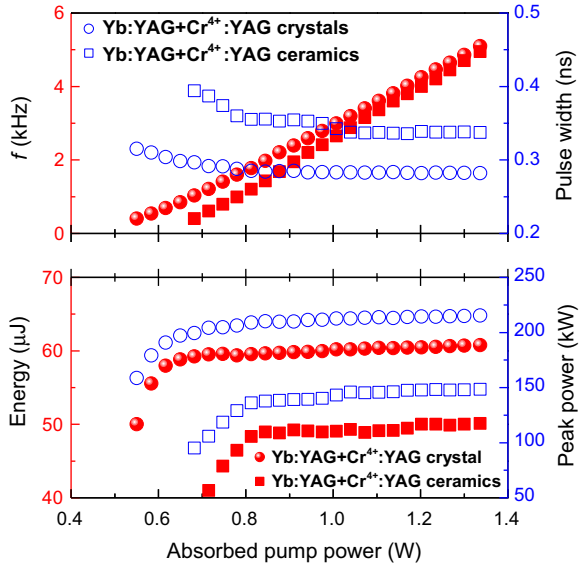

Fig. 7. Pulse characteristics (repetition rate, pulse width, pulse energy and peak power) of passively Q-switched Yb:YAG/C^{4+}:YAG microchip lasers as a function of absorbed pump power.

lasers decreases with absorbed pump power at low pump power levels and tends to keep constant at high pump power levels. Pulse energy increases with absorbed pump power and tends to keep constant at high pump power levels. The highest pulse energy of 61 μJ and 50 μJ was achieved with Yb:YAG/Cr^{4+}:YAG all-crystal combination and all-ceramics combination, respectively. Peak power of passively Q-switched Yb:YAG/Cr^{4+}:YAG microchip lasers exhibits the same tendency as those of pulse energy. The overall best laser performance (highest peak power) in passively Q-switched Yb:YAG/Cr^{4+}:YAG microchip lasers achieved by using Yb:YAG/Cr^{4+}:YAG all-crystals combination.

The polarization states of passively Q-switched Yb:YAG/Cr^{4+}:YAG microchip lasers with all-crystal and all-ceramic combinations were investigated by measuring the output power after polarizer. By rotating the Yb:YAG/Cr^{4+}:YAG combination, the polarization states of these lasers do not change, only the polarization directions are changed by arranging Yb:YAG or Cr^{4+}:YAG. Rotating any one of sample does not affect the polarization states and no stronger influence on the polarization was observed. Fig. 8 shows the typical polarization states of Yb:YAG/Cr^{4+}:YAG microchip lasers with all-crystals and all-ceramics combinations. Yb:YAG/Cr^{4+}:YAG all-crystals combination exhibits linearly polarized state with extinction ratio of greater than 300:1. While Yb:YAG/Cr^{4+}:YAG

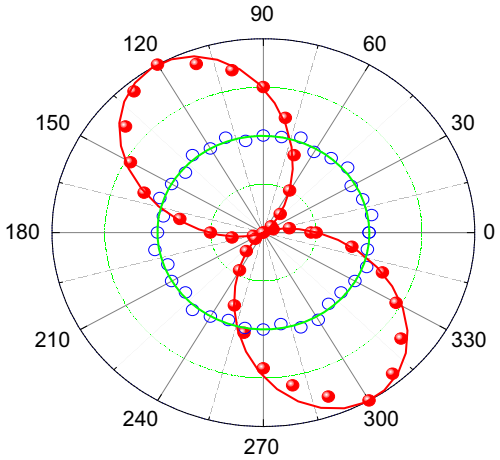

Fig. 8. Polarization states of passively Q-switched Yb:YAG/Cr^{4+}:YAG microchip lasers. The solid lines show the sine function fitting of the experimental data.

all-ceramics combination exhibits circular polarized state. The extinction ratios of linearly polarized laser for Yb:YAG/Cr^{4+}:YAG all-crystals combination decrease a little with increase of the pump power, no significant decrease of the extinction ratio was observed at the maximum pump power used here, which shows that the thermal effect under current available pump power is not strong enough to induce sufficient birefringence and depolarization for Yb:YAG crystals. However, we did observe the thermal effect under high pump power level for cw Yb:YAG microchip lasers [33], therefore, the thermal effect induced birefringence and depolarization should be considered in high power pumped passively Q-switched Yb:YAG/Cr^{4+}:YAG microchip lasers.

The output beam transverse intensity profiles were also monitored in all the pump power range for continuous-wave and Q-switched lasers. The output beam profile is close to TEM_{00} mode. Near-diffraction-limited beam quality with M^2 of less than 1.1 was achieved in these microchip lasers with Yb:YAG ceramics or crystals as gain media in the available pump power range.

4. Conclusions

In conclusion, investigations of continuous-wave and Q-switched microchip laser performance were done for Yb:YAG ceramics and crystals doped with 10 at.% Yb. Efficient continuous-wave and Q-switched laser performance was obtained for both Yb:YAG crystal and ceramic. For different transmissions of output couplers, Yb:YAG ceramics give the same continuous-wave laser characteristics as that of Yb:YAG crystal, except the higher pump power threshold. The laser performance of Yb:YAG crystal is better than that of Yb:YAG ceramic. The lasers oscillate at multi-longitudinal-mode owing to the broad emission spectra of Yb:YAG. The strong reabsorption and gain curve change under high intracavity laser intensity play important roles on the red-shift of the output laser wavelength. Efficient passively Q-switched Yb:YAG/Cr^{4+}:YAG microchip lasers with sub-nanosecond pulse width and peak power of over 150 kW have been achieved. Linearly polarized lasers were obtained in Yb:YAG/Cr^{4+}:YAG all-crystals combination, while circularly polarized lasers were achieved in Yb:YAG/Cr^{4+}:YAG all-ceramics combination.

Acknowledgements

This work was supported by Program for New Century Excellent Talents in University (NCET-09-0669), SRF for ROCS, SEM, a grant from the Ph.D. Programs Foundation of Ministry of Education of China (20100121120019), the Fundamental Research Funds for

the Central Universities (2010121058), and by the Russian Foundation for Basic Research, as well as by the Program "Femtosecond physics and new optical materials" of Presidium of Russian Academy of Sciences.

References

[1] W.F. Krupke, IEEE J. Sel. Top. Quantum Electron. 6 (2000) 1287–1296.
[2] G.A. Bogomolova, D.N. Vylegzhanin, A.A. Kaminskii, Sov. Phys. JETP 42 (1976) 440–446.
[3] L. Dobrzycki, E. Bulska, D.A. Pawlak, Z. Frukacz, K. Wozniak, Inorg. Chem. 43 (2004) 7656–7664.
[4] J. Dong, A. Shirakawa, S. Huang, Y. Feng, T. Takaichi, M. Musha, K. Ueda, A.A. Kaminskii, Laser Phys. Lett. 2 (2005) 387–391.
[5] J. Lu, M. Prabhu, J. Song, C. Li, J. Xu, K. Ueda, A.A. Kaminskii, H. Yagi, T. Yanagitani, Appl. Phys. B 71 (2000) 469–473.
[6] J. Lu, M. Prabhu, J. Song, C. Li, J. Xu, K. Ueda, H. Yagi, T. Yanagitani, A.A. Kaminskii, Jpn. J. Appl. Phys. 40 (2001) L552–L554.
[7] J. Lu, K. Ueda, H. Yagi, T. Yanagitani, Y. Akiyama, A.A. Kaminskii, J. Alloys Compd. 341 (2002) 220–225.
[8] J. Dong, A. Shirakawa, K. Ueda, H. Yagi, T. Yanagitani, A.A. Kaminskii, Appl. Phys. Lett. 89 (2006) 091114.
[9] T. Takaichi, H. Yagi, J. Lu, A. Shirakawa, K. Ueda, T. Yanagitani, A.A. Kaminskii, Phys. Status Solidi (a) 200 (2003) R5–R7.
[10] T. Yanagitani, H. Yagi, Y. Hiro, Japan Patent 10-101411, 1998.
[11] H. Yagi, T. Yanagitani, K. Yoshida, M. Nakatsuka, K. Ueda, Jpn. J. Appl. Phys. 45 (2006) 133–135.
[12] J. Dong, K. Ueda, A. Shirakawa, H. Yagi, T. Yanagitani, A.A. Kaminskii, Opt. Express 15 (2007) 14516–14523.
[13] J. Dong, A. Shirakawa, K. Takaichi, K. Ueda, H. Yagi, T. Yanagitani, A.A. Kaminskii, Electron. Lett. 42 (2006) 1154–1156.
[14] J. Dong, A. Shirakawa, K. Ueda, H. Yagi, T. Yanagitani, A.A. Kaminskii, Appl. Phys. Lett. 90 (2007) 131105.
[15] J. Dong, A. Shirakawa, K. Ueda, H. Yagi, T. Yanagitani, A.A. Kaminskii, Appl. Phys. Lett. 90 (2007) 191106.
[16] E.C. Honea, R.J. Beach, S.C. Mitchell, J.A. Sidmore, M.A. Emanuel, S.B. Sutton, S.A. Payne, P.V. Avizonis, R.S. Monroe, D. Harris, Opt. Lett. 25 (2000) 805–807.
[17] T.S. Rutherford, W.M. Tulloch, E.K. Gustafson, R.L. Byer, IEEE J. Quantum Electron. 36 (2000) 205–219.
[18] A. Giesen, H. Hugel, A. Voss, K. Wittig, U. Brauch, H. Opower, Appl. Phys. B 58 (1994) 365–372.
[19] C. Stewen, K. Contag, M. Larionov, A. Giessen, H. Hugel, IEEE J. Sel. Top. Quantum Electron. 6 (2000) 650–657.
[20] J. Dong, K. Ueda, Laser Phys. Lett. 2 (2005) 429–436.
[21] H. Yin, P. Deng, F. Gan, J. Appl. Phys. 83 (1998) 3825–3828.
[22] P. Yang, P. Deng, Z. Yin, J. Lumin. 97 (2002) 51–54.
[23] H. Qiu, P. Yang, J. Dong, P. Deng, J. Xu, W. Chen, Mater. Lett. 55 (2002) 1–7.
[24] J. Dong, A. Shirakawa, K. Ueda, A.A. Kaminskii, Appl. Phys. B 89 (2007) 359–365.
[25] D.S. Sumida, T.Y. Fan, Opt. Lett. 19 (1994) 1343–1345.
[26] J. Dong, A. Shirakawa, K. Ueda, H. Yagi, T. Yanagitani, A.A. Kaminskii, Opt. Lett. 32 (2007) 1890–1892.
[27] J. Dong, K. Ueda, H. Yagi, A.A. Kaminskii, Z. Cai, Laser Phys. Lett. 6 (2009) 282–289.
[28] J. Dong, A. Rapaport, M. Bass, F. Szipocs, K. Ueda, Phys. Status Solidi (a) 202 (2005) 2565–2573.
[29] W. Kochner, Solid State Laser Engineering, Springer-Verlag, Berlin, Germany, 1999.
[30] J. Dong, M. Bass, Y. Mao, P. Deng, F. Gan, J. Opt. Soc. Am. B 20 (2003) 1975–1979.
[31] J. Kong, D.Y. Tang, J. Lu, K. Ueda, Opt. Lett. 29 (2004) 65–67.
[32] H. Eilers, K.R. Hoffman, W.M. Dennis, S.M. Jacobsen, W.M. Yen, Appl. Phys. Lett. 61 (1992) 2958–2960.
[33] J. Dong, A. Shirakawa, K. Ueda, Appl. Phys. Lett. 93 (2008) 101105.